Research Inventy: International Journal of Engineering And Science
Vol.14, Issue 12 (December 2024), PP 76-86
Issn (e): 2278-4721, Issn (p):2319-6483, www.researchinventy.com

The hovering of a balloon-multicopter with a special assembly scheme

Tran Duy Duyen
Air Defense – Air Force Academy, Viet Nam
**Corresponding Author Email: duyduyen85@gmail.com*

Abstract: *The balloon-multicopter or ballooncopter is a new flight vehicle type that combines the advantages of a balloon (long flight, high lift without losing energy, environmental friendliness) and those of a multicopter/ multirotor device (VTOL capability, easy to control both the attitude and the CG position when hovering and flying at low speed in windy conditions). The ballooncopters, esspecially with reduced-drag-shaped balloon, can be highly effective in different fields such as long-time monitoring, tourism and transportation to the areas that are difficult to reach by conventional means. This article deals with ballooncopters that have a special solution to assemble a multicopter with the balloon and payload compartment as a scheme of two seriesly hung pendulums compared with the known scheme without the 3-rd joint. The suggested assembly scheme many times reduces the necessary power of the rotors when needed to tilt the thrust vector in windy conditions that makes possible to maintaine the hovering point coordinates and desired flight path The new assembly scheme requires balance and stability considerations when flying in windy conditions.The problems and their solutions were presented in the recently published papers This article will deal with the dynamics of hoveringm of the ballooncopter with the two assamble schemes under action of a step-form wind gust that shows quantatively the advantage of the suggested assamble scheme. The hovering flight is simulated with an autopilot that asigned for maintaining the desired coordinates.*

Keywords: *Balloon-multicopter, balloon, ballooncopter with special asamble sheme, possibility to maintaine desired coordinates, windy conditions.*

Date of Submission: 22-12-2024 Date of acceptance: 02-01-2025

I. INTRODUCTION

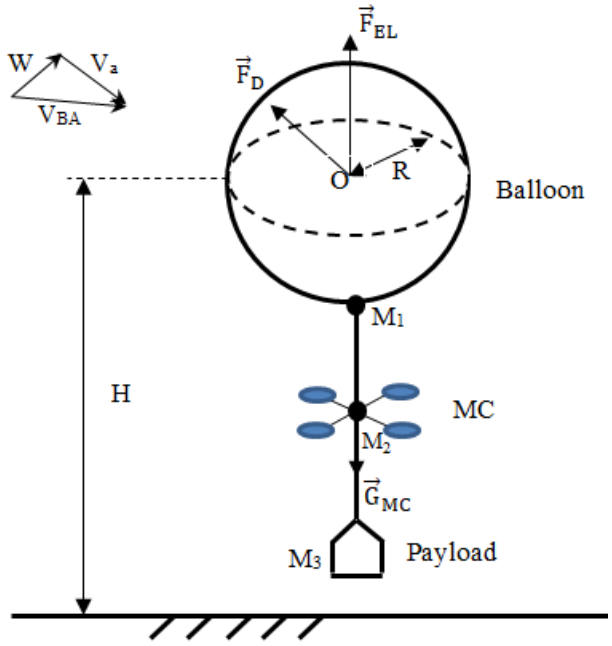

Figure 1 Overall layout of a ballooncopter

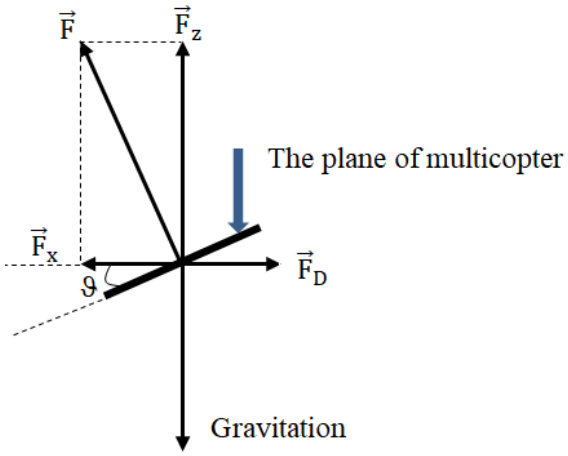

Figure 2 The components of thrust vector $\vec{F}$: F_z (for weight balance) and F_x (for aerodynamic force $\vec{F}_D$ balance)

Fig.1 shows the overall layout of a ballooncopter [1] consisting of 3 main parts: the balloon, the multicopter and the payload. The balloon is not necessarily spherical, but for the scope of this article we only consider the spherical balloon. The ballooncopter is a new flight vehicle type combining the advantages of a balloon (long flight, high lift without losing energy, environmental friendliness) with multicopter (VTOL capability, easy to control both attitude and the CG position when hovering and flying at low speed, easy manufacture). This idea has been suggested for a long time [2], four-rotor rotastat [3], however, the authors have proposed to *rigidly* attach the balloon (with payload compartment) to the multicopter, so it is still necessary to use high power rotors to tilt the whole ballooncopter with balloon and payload compartment for controlling the thrust vector. This article mentions that the ballooncopter has a solution to assemble the multicopter with the balloon and the payload compartment due to 2 joints forming a scheme of 2 seriesly hung pendulums (Fig. 3), which allows to significantly reduce the necessary power of the rotors when tilting the thrust vector. On the fig.3 the joint M_2 constructively splits into the two very close each to other upper joint M_{2t} and the lower joint M_{2d} to avoid any modification of the existing construction of the multicopter. In the further considerations we'll make no difference of the joints M_{2t} and M_{2d} and assume them to be a single joint M_2, neclecting the distance between them The joint M_2 to hang the payload is frictionless in the cases of tourism or transportation versions, but in case of monitoring version the joint must intentionally to have signìicant friction moment to damp the undesired oscillation of the payload.

This new assembly scheme requires balance and stability considerations when flying with and without wind turbulence. This article will deal with these problems in the scope of longitudinal motion.

The coefficient of aerodynamic force was taken for the case of the smooth sphere C_x=0.3 [4] at the number Re=3.10^6.

Fig. 2 introduces the known principle of controlling the movement of the multicopter center of mass by the thrust vector $\vec{\mathbf{F}}$: when tilting the vector $\vec{\mathbf{F}}$ to a pitch angle ϑ (fig.2), a force $\vec{\mathbf{F}}_\mathbf{z}$ will be generated to balance the gravity and create a force $\vec{\mathbf{F}}_\mathbf{x}$ to balance the aerodynamic force caused by the wind (or caused by the movement of the multicopter relative to the air). Thus, in order to control the ballooncopter, it is necessary to tilt the force vector $\vec{\mathbf{F}}$, that is, tilt the multicopter according to the pitch angle ϑ. The yaw angle in the ground reference system OXYZ also needs to be controlled but will be mentioned later (in the article where the lateral motion is concerned). The suspension rod is nescesary to be rigid to torque moment that ensures the balloon together the GPS-guided multicopter in landing with following moring on the ground. The connection scheme of the ballooncopter allows almost freely tilting the multicopter to create forces whitch are needed to control the trajectory (coordinates of the center of mass) in the ground reference system OXZ without tilting both the massive payload compartment and the suspension rod M_1M_2 with the massive balloon.

During take-off and landing, it is necessary to increase/decrease the component $\vec{\mathbf{F}}_\mathbf{z}$ (fig. 2) by increasing/decreasing the rpm of the rotors to increase/decrease the total force $\vec{\mathbf{F}}$**.** It should be emphasized that since the balloon have helium gas that lifts about 95% of the total weight, while the multicopter only takes care of residual gravity ΔG about 5% of the total weight when it flies at a constant altitude (for VASA-3M, F_z= 200N), for take-off and landing and altitude control, the F_z force will be variated in the range of 0 to 17% (for VASA-3M if using multicopter U30K then F_{max} = 700N) to ensure that the vertical speed is not too slow when climbing or not too quick when gliding.

The ballooncopter does not have a separate propulsion system to fly forward, so it is to use the multicopter tilted forward as shown in fig. 2, of course ballooncopter can't fly fast. For VASA-3M, if agricultural multicopter U30K (F_{max} =700N) is used and is modified to hybridize with a balloon with diameter D=9m, the cruise flight speed is only about 15km/h (50% capacity of the rotors, so not to run out of the batteries), similarly to riding a bicycle.

Now the static balance and the static stability of this ballooncopter scheme will be considered at a rectilinear horizontal uniform flight without wind, then later the dynamic problem of flight of the ballooncopter will be considered.

II. THE STATIC BALANCE, THE STATIC STABILITY AND SOME QUALITATIVE ANALYSIS

The static equilibrium of the ballooncopter parts must be analyzed, and if the equilibrium is stable, that is, if the displacements of the points M_1' and M_2 in Fig.1, may be too large.

At a rectilinear horizontal uniform flight without wind, due to the force $\vec{\mathbf{F}}_\mathbf{x}$, the suspension rod L_1 at the bottom of the balloon will deviate by an angle γ_{12}, the point M_2 will be displaced in the direction of flight (fig. 4). The external forces acting on the ballooncopter must be balanced in the ground reference system:

$$F_{EL} = G_{T-PL} + G_{MC} - F_z \quad (1)$$

$$F_x = F_{Dx} \quad (2)$$

According to the rule of three concurrent forces, the vector $\vec{\mathbf{T}}_1$ – reaction of the suspension rod L_1 (line segment M'_1M_2) will have an action line that goes through the center point O, because the vectors $\vec{\mathbf{F}}_{\mathbf{Dx}}$ and $\vec{\mathbf{F}}_{\mathbf{EL}}$ both create a resulting force at the center O (due to symmetry of balloon). Hence, the angle γ_0 will be:

$$\gamma_0 = \text{arctg}\left(\frac{F_{DX}}{F_{EL}}\right) \tag{3}$$

On the other hand, the suspension rod L_1 must also lie in the radial direction through the center O of the sphere when the system is in equilibrium, i.e.:

$$\gamma_0 = \gamma_{12} \tag{4}$$

For VASA-3M at a rectilinear horizontal uniform flight with V=15 km/h the angles are very small ($\gamma_0 = \gamma_{12} = 3.1^o$).

We will consider if this angular position of the pendulum L_1 is stable equilibrium. It is clear that when M_2 shifts to the position M_2' or M_2'' (or $\Delta\gamma_{12}$ appears) an unbalanced moment ΔM always appears acting to liquidate the deviation $|\Delta\gamma_{12}| \rightarrow 0$ (fig. 4):

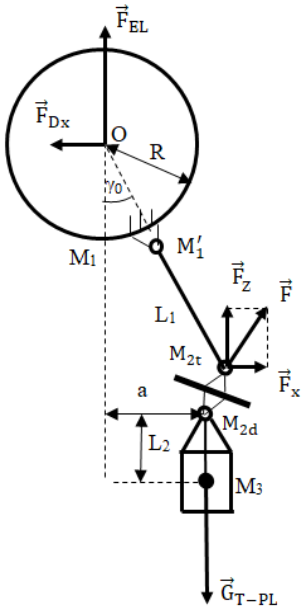

Figure 3 The scheme of the balloncopter connecting 3 main parts according to the scheme of 2 seriesly hung pendulums at a rectilinear horizontal uniform flight

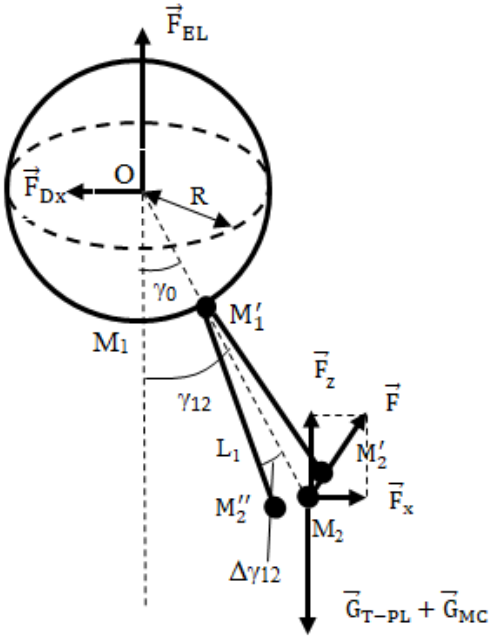

Figure 4 Static stability of the point M_2 (or of angle γ_{12})

It is clear that at rectilinear horizontal uniform flight the payload lies vertically and the angle γ_{22}=0 and it is a stable equilibrium.

The horizontal displacement a of the multicopter relative to the vertical line (fig. 3) at rectilinear horizontal uniform flight without wind may be deduced from balance of the external moments relative to the point M_1' (assuming the angles to be small enough):

$$\mathbf{a} = \frac{F_x}{K_1} \tag{5}$$

$$K_1 = \frac{G_{T-PL} + G_{MC} - F_z}{L_1 + R} \tag{6}$$

That is, the pendulum mechanism L_1 acts almost like a spring with a stiffness K_1. When increasing the angle γ_{12} the lever arm of the force $(G_{T-PL} + G_{MC} - F_z)$ also increases, so that the appearing an unbalanced moment will decrease the angle γ_{12} and contrary. Thus, the equilibrium position of the angle $\gamma_{12} = \gamma_0$ of the pendulum L_1 is a stable position. And the coefficient K_1 can be considered as the static stability of the balloncopter (similar to the distance from the center of mass to the aerodynamic center of a fixed-wing aircraft).

Note: force $F_z \ll (G_{T-PL} + G_{MC})$ so K_1 is generally >0. From the expression (6) for calculating the value of K_1, we see that "spring stiffness" (static stability of the balloncopter) is directly proportional to the

weight of the hanging objects and inversely proportional to the total length of the suspension rod L_1 and the radius R.

It is nescessary that the static stability of point M_1' (or angle γ_0) also to be considered (fig. 5). If a small deviation $\Delta\gamma_0$ appears , it causes an unbalanced moment ΔM to recover the angle γ_0 or to liquidate the $\Delta\gamma_0$. It means that the position of M_1' on the balloon envelope is also stable.

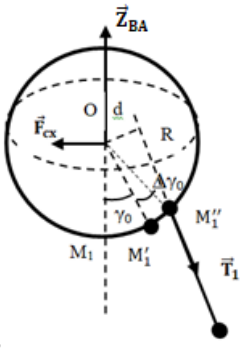

s

Figure 5 The static stability of the point M_1'

Of course, when multicopter motion has acceleration (e.g., while changing the vector $\vec{\mathbf{F}}$) there will be a pendulum effect of the payload hung to the multicopter at point M_2 by a joint and the angle $\gamma_{22}\neq 0$. When point M_2 has forward acceleration ($\ddot{x}_{MC} > 0$) then mass $m_{T\text{-}PL}$ ($m_{T-PL} = m_{PL} + m_{S-PL} + m_{BL}$) that is about 350kg for VASA-3M will move backwards, creating a significant braking force to reduce acceleration $\ddot{x}_{MC}$, contrarily, when $\ddot{x}_{MC}<0$ the same process happens but in the opposite direction. Through the above qualitative analysis, one can conclude that the ballooncopter will be stable even when the motion has acceleration.
In short, qualitative analysis shows that the ballooncopter can perform a stable flight.

III. MATHEMATICAL MODEL OF LONGITUDINAL MOTION OF THE BALLOONCOPTER

3.1 The main assumptions

The attitude (pitch angle) control system of the multicopter is assumed to be an ideal control system that means the attitude control of the multicopter is assumed to be performed instantaneously without errors. This assumption allows to neglect the rotation and the inertia moment of the multicopter in this dynamic problem. So the multicopter may be considered as a particle of mass m_{MC} with its translational motion without rotation.

The rotation of balloon around its center O may be ignored since its significant inertia moment relative to the center compared with unbalanced external moment acting on the sphere, and one may consider only its translational motion, so that the balloon may be considered as a particle of mass m_{BA}. The hung payload as a pendulum that will oscillate around the point M_2 may be considered as a pendulum comprising a particle of mass $m_{T\text{-}PL}$ hung by a rigid rod with length L_2 (radius of inertia of payload).

Thus, the whole ballooncopter may be considered as a mechanical system comprising 3 particles of mass m_{BA}, m_{MC} and m_{T-PL} connected by joints and rods in which the balloon, multicopter and payload are assumed to be considered as concentrated masses at points O, M_2, M_3 respectively.

When considering the aerodynamic force, the focus is only done on the aerodynamic drag of the sphere $\vec{\mathbf{F}}_{\mathbf{D}}$, and the aerodynamic drag of the multicopter and that of the payload compartment can be ignored because the cross-sectional areas of these parts is only a few percent of that of the balloon. When calculating the aerodynamic force acting to the sphere, the difference of the velocity field acting at different points of the sphere is ignored, the field is considered as a uniform field with one and the same velocity value corresponding to the center O of the sphere.

The point M_1' is assumed always to be in a straight line with the points O and M_2 or we always have the expesion $\gamma_0=\gamma_{12}$.

The link rods of the masses are assumed to be weightless and absolutely rigid.

Only the longitudinal motion of the balloncopter is considered that is balloncopter flying straightly in the windless/tailwind/headwind and vertical wind conditions. In the case of monitoring version we will consider the particular flight : hovering.

With the above mentionned assumptions, we have a model of dynamics of the balloncopter in the longitudinal motion shown in fig.6.

Thus one must consider two problems : the first one is a problem without friction and the second one is problem with friction. The problems are further presented in more details as follows.

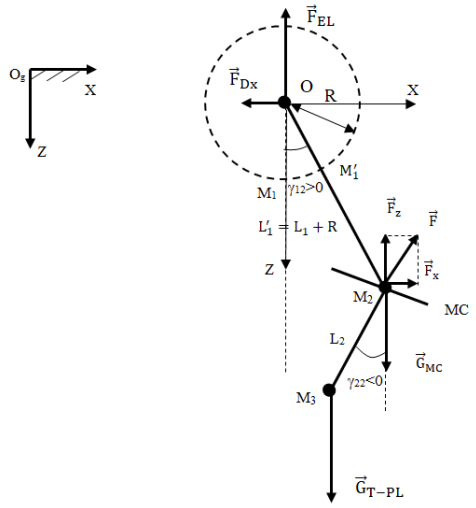

Figure 6. The moving reference system OXZ and the fixed reference system O_gXZ for the 3-body mechanical system: balloon, multicopter and payload in the longitudinal motion

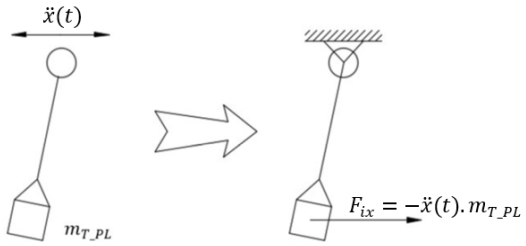

Figure 7. Converting the pendulum problem with moving hang joint to the problem with fixed hang joint

3.2 The problem without friction

For the shown mechanical system with constraints one can establish a system of differential equations of motion using the method of Lagrange equations type II [5] as following:

For the 4-DOF mechanical system the fully generalized coordinates were chosen as follows:

$q_1 = X_{BA}, q_2 = Z_{BA}, q_3 = \gamma_{12}, q_4 = \gamma_{22}$ ($\gamma_{12}, \gamma_{22} > 0$ when turning counter-clockwise).

Action forces acting on the system: $P_{ac}, G_{KC}, G_{MC}, G_{tong\_TCI}, F_x, F_z, F_{Dx}, Ff_{Dz}$

Where: $G_{BA} = m_{BA}.g, G_{MC} = m_{MC}.g, G_{T-PL} = m_{T-PL}.g$

$$F_{Dx} = \text{sign}(V_{xBA} - W_x)0.5C_x\rho_a S(V_{xBA} - W_x)^2 \quad (7)$$

$$F_{Dz} = \text{sign}(V_{zBA} - W_z)0.5C_z\rho_a S(V_{zBA} - W_z)^2 \quad (8)$$

Kinetic energy: $T = T_{BA} + T_{MC} + T_{PL}$

$$T_{BA} = \frac{1}{2}m_{BA}(\dot{X}_{BA}^2 + \dot{Z}_{BA}^2);\ T_{MC} = \frac{1}{2}m_{MC}(\dot{X}_{MC}^2 + \dot{Z}_{MC}^2);\ T_{PL} = \frac{1}{2}m_{T-PL}(\dot{X}_{PL}^2 + \dot{Z}_{PL}^2); \quad (9)$$

$$\begin{cases} X_{M2} = X_{MC} = X_{BA} + L_1'\sin\gamma_{12} \\ Z_{M2} = Z_{MC} = Z_{BA} + L_1'\cos\gamma_{12} \end{cases}; \begin{cases} X_{PL} = X_{MC} + L_2\sin\gamma_{22} \\ Z_{PL} = Z_{MC} + L_2\cos\gamma_{22} \end{cases} \quad (10)$$

Generalized force: Total power of the active forces

$$\sum CS = -F_{Dx}\dot{X}_{BA} - (P_{ac} - G_{BA} - F_{Dz})\dot{Z}_{BA} + F_x\dot{X}_{MC} - (F_z - G_{MC})\dot{Z}_{MC} + G_{T-PL}\dot{Z}_{PL} \quad (11)$$

The partial derivatives of the generalized forces to the corresponding generalized coordinates:

$$Q_1 = \frac{\partial\sum CS}{\partial\dot{X}_{BA}};\ Q_2 = -\frac{\partial\sum CS}{\partial\dot{Z}_{BA}};\ Q_3 = \frac{\partial\sum CS}{\partial\dot{\gamma}_{12}};\ Q_4 = \frac{\partial\sum CS}{\partial\dot{\gamma}_{22}} \quad (12)$$

Substitute the above expressions into the Lagrange equations of type II

$$\frac{d}{dt}\left(\frac{\partial T}{\partial\dot{q}_i}\right) - \frac{\partial T}{\partial q_i} = Q_i, \qquad i = 1 \dots 4 \quad (13)$$

Then one can set up a system of differential equations for the motion of the system. The process of loading input data, calculating the above formulas and solving the system (by numerical method) is done in MAPLE. Thus, it will be possible to build a software to calculate and determine the motion parameters of the mechanical system, this software needs to be tested qualitatively and quantitatively to confirm the reliability, which will be presented in the following paragraph.

Testing the software

We can test qualitatively by increasing or decreasing some parameters and also quantitatively for a few particular cases with known solutions in advance. For example, the authors tested qualitatively as follows: changing tailwind/headwind speed, air density, diameter of the balloon, control force of the multicopter, etc. And all simulation results were changed in appropriate directions. Quantitative testing for some particular cases such as: test of asymptotic cases, for example for $C_x \to 0$, L_1, $L_2 \to \infty$, then the results are also asymptotically approach to the known limits.

It is a fact that most of the results of numerical solutions can only be *tested qualitatively* and tested *quantitatively in a few special cases.* Therefore, confirming the general correctness of mathematical model and software often requires physical tests that are complicated and sometimes dangerous, which are sometimes more difficult and expensive than the development of mathematical model and software.

In this problem, in addition to the qualitative test, we can use the change in the kinetic energy of the system and the work of the external forces to quantitatively check the calculation results. Specifically, according to theoretical mechanics, there is the kinetic energy variation theorem of a mechanical system: *"The time derivative of the kinetic energy of a mechanical system is equal to the sum of the powers of the internal forces and external forces acting on the system"*. Applying to the dynamic model, according to this theorem (the work of the internal forces is zero), we have the following expression:

$$\frac{dT}{dt} = -F_{Dx}\dot{X}_{BA} - (P_{ac} - G_{BA} + F_{Dz})\dot{Z}_{BA} + F_x\dot{X}_{MC} - (F_z - G_{MC})\dot{Z}_{MC} + G_{T-PL}\dot{Z}_{PL} \quad (14)$$

Performing the calculation to check the formula (14) in MAPLE we see that this formula is satisfied at every time step.

3.3 The problem with friction

In the problem with friction we'll consider the oscillations of the lower pendulum separately, with oscillating hang joint when the maximal oscillations of the hang joint have been obtained from the first problem without friction.assuming that there is no invers action to the whole 3-body mechanical system from the damped payload oscillations.

. The joint M_2 (to hang the payload) is considered with intentional friction. In this problem static friction is ignored because in case if the static friction is not neglected one obtains more damped oscillations Thus, these assumptions allow to obtain the most sever case, that is the highest estimation of the oscillations.

As known, to create the friction moment M_{frx} in the joint, one must create the friction force F_{fr} of sliding surfaces on a finite radius r, and the moment always acts against the rotation, that is

$$M_{frx} = -k_{fr} N r \operatorname{sign}(\dot{\gamma}_{22}) \quad (15)$$

The first problem without friction of the whole 3-body mechanical system gives the accelleration $\ddot{x}(t)$ that will be as input data for the oscillation pendulum problem in the planes M_2XZ (fig.7) acting as inertia force $F_{ix} = -\ddot{x}(t)m_{T-PL}$ on the arm L_2 and creating moment M_{ix}. One can establish an ordinary differential equation for the classical pendulum relative to angle γ_{22} with external moments $M_{ix} = F_{ix}.L_2$, friction moment M_{frx} (15) and gravity moment $gm_{T-PL}L_2\gamma_{22}$ (The diference bettween CG and center of inertia is neglected and the angle γ_{22} was assumed to be small angle):

$$-L_2\ddot{x}(t)m_{T-PL} - k_{fr}Nr\operatorname{sign}(\dot{\gamma}_{22}) - gm_{T-PL}L_2\gamma_{22} = L_2^2 m_{T-PL}\ddot{\gamma}_{22} \quad (16)$$

To overcome the dificulties in numerical solution the function sign(x) discontinued at x=0 is approximated by a continued function $\frac{2}{\pi} arctg(10x)$.

3.4 Calculations and discussions

Calculation results will be shown for two versions of hypothetical balloon copter in the presence of wind disturbances. The first balloon copter is designed for tourism and the second one is for momitoring that requires joint with intentional friction to damp undesired small oscillations. The second problem calculations results are similar to those of the tourist version in straight flight of the first problem and are not shown. There

were shown only for hoverring flight The hovering flight is simulated with an autopilot which is selected to ensure no oscillations of the accelerations of the multicopter CG.

Tourist version

In this version the input and initial data will be:

D=9m, H_0=205.5m, V_{0xBA}=4m/s, V_{0zBA}=0.

C_x=C_z=0.3, g=9.81m/s^2, L_1=1m, L_2=1.5m.

m_{PL}=230kg, m_{SBA}=50kg, m_{MC}=15kg, $m_{S\text{-}PL}$=40kg, m_{BL}=81.55kg, ρ_a=1.16kg/m^3, ρ_{He}=0.16 kg/m^3.

$$S = \pi R^2, VOL = \frac{4\pi R^3}{3}, m_{He} = \rho_{He} VOL,\ m_{BA} = m_{SBA} + m_{He}.$$

$$m_{T-PL} = m_{PL} + m_{S-PL} + m_{BL},\ m_T = m_{BA} + m_{MC} m_{T-PL}.$$

$$P_{ac} = VOL\rho_a g.$$

$$F_{Dx0} = 0.5 C_x \rho_a S V_{0xBA}^2,\ F_{Dz0} = 0.$$

$$F_x = F_{Dx0},\ F_z = F_{Dz0};\ \gamma_{120} = \text{acrtg}\left(\frac{F_{Dx0}}{F_{EL}}\right);\ \gamma_{220} = 0.$$

Time of investigation: t_{tf} =30s.

$$X_{BA}(0) = 0, \dot{X}_{BA}(0) = V_{0xBA}, Z_{BA}(0) = H_0,\ \dot{Z}_{BA}(0) = 0, \gamma_{12}(0) = \gamma_{22}(0) = 0\ , \dot{\gamma}_{12}(0) = \dot{\gamma}_{22}(0) = 0.$$

For the case of a rectilinear horizontal uniform flight without wind, encountering step disturbance (headwind)

$$\begin{cases} W = W_x = 0 \text{ when } t < 6s \\ W = W_x = -3m/s \text{ when } t > 6s \end{cases}$$

we have some calculation results as follows (fig. 8, 9, 10):

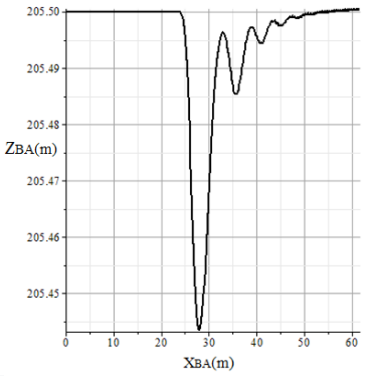

Figure 8. Trajectory of the balloocopter when encountering headwind W_x=-3m/s

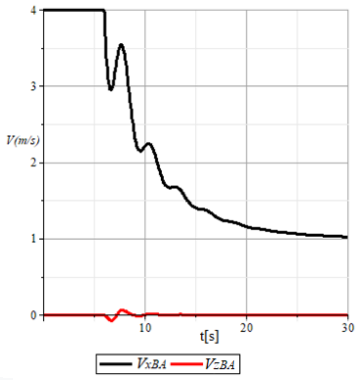

Figure 9. The velocity of the balloocopter in the X, Z directions when encountering headwind W_x=-3m/s

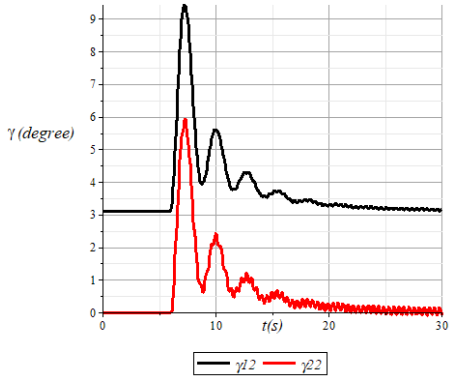

Figure 10. The oscillation angles γ_{12} ,γ_{22} of suspension objects when encountering headwind W_x=-3m/s

Comment: The small undamped oscillations are not important in case ò tourist version, furthermore if the model includes disipative factors (drag and friction), though very small, the oscillations is to be damped completly maybe after a long time.

For the case of a rectilinear horizontal uniform flight without wind, encountering step disturbance (tailwind)

$$\begin{cases} W = W_x = 0 \text{ when } t < 6s \\ W = W_x = 3m/s \text{ when } t > 6s \end{cases}$$

we have some results of calculating the motion parameters of the mechanical system as follows (fig. 11,12,13):

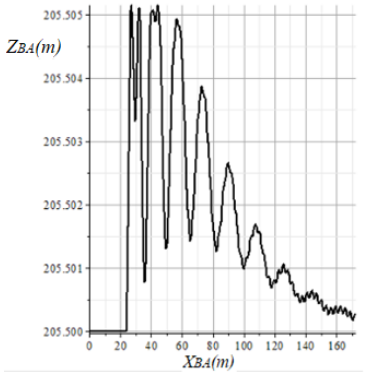

Figure 11. Trajectory of the balloncopter when encountering tailwind W_x=3m/s

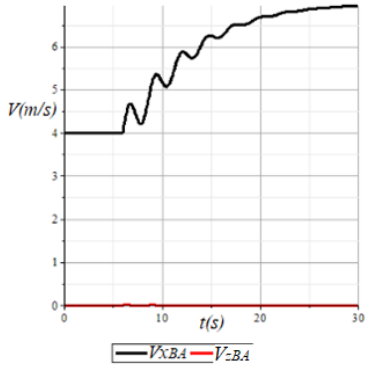

Figure 12. The velocity of the balloncopter in the x, z directions when encountering tailwind W_x=3m/s

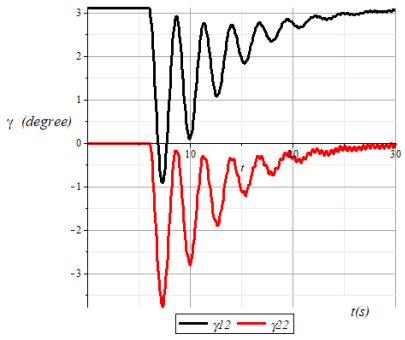

Figure 13. The oscillation angles γ_{12},γ_{22} of suspension objects when encountering tailwind W_x=3m/s

Comment: Similar to comment for the fig.10

To confirm the ability of the balloncopter to fly in wind turbulence (with changes in space-position on the OX axis), we consider a sinusoidal wind symmetric oscilation form modified from JAR-VLA standards [6].

$$\begin{cases} W = W_z = 0 \text{ when } t < 6s \\ W = W_z = 7.62\cos\left(\dfrac{2\pi X_{BA}}{\lambda}\right) m/s \text{ when } t > 6s \end{cases}$$

Here are some results in the case of the balloncopter when flying into an area with turbulence with resonant wavelength λ=1.8 m (fig. 14,15,16):

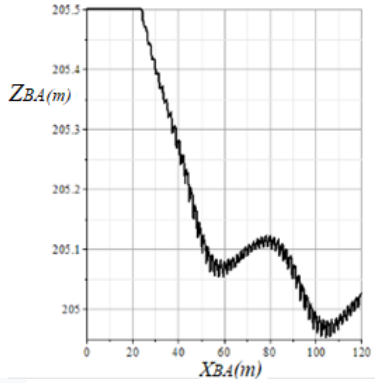

Figure 14. Trajectory of the balloncopter when encountering the resonant sinusoidal vertical wind

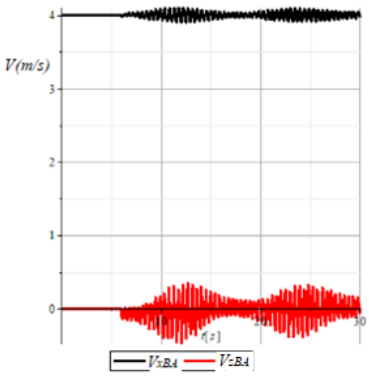

Figure 15. The velocity of the balloncopter in the X, Z directions when encountering the resonant sinusoidal vertical wind.

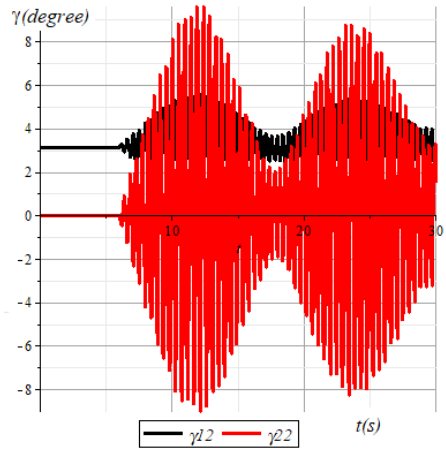

Figure 16. The oscillation angles γ_{12},γ_{22} of suspension objects when encountering the resonant sinusoidal vertical wind

Comment: Even in the presence of resonant disturbances (the most sever but very rarely) the flight oscillations of the hypothetical ballooncopter with the above suggested parameters remains small enough and acceptable for tourism.

Monitoring version (with friction)

In this version the input, initial data and the calculation results only were shown for hovering flight.

D=5m; H_0=203.5m; V_{0zBA}=0; C_x=C_y=0.3; g=9.81m/s^2; L_1=1m; L_2=1,5m. $m_{T\text{-}PL}$=20kg; m_{SBA}=16kg; m_{MC}=14kg; $m_{S\text{-}PL}$=4kg; m_{BL}=4kg (ballast load); ρ_a=1.16kg/m^3; ρ_{He}=0.16 kg/m^3. R=D/2=2,5m; S=πR^2=19.62m^2; VOL=(4πR^3)/3=65.4m^3; $m_{He}=\rho_{He}VOL$=10.5kg; $m_{BA}=m_{SBA}+m_{He}$=26.5kg; $m_{T\text{-}PL}=m_{PL}+m_{S\text{-}PL}+m_{BL}$; $m_T=m_{BA}+m_{MC}+m_{T\text{-}PL}$. $P_{ac}=VOL\rho_a g$.

Coefficient of sliding friction K_{fr}=0.94, aluminium/aluminium [7], normal reaction of sliding surfaces N=g.$m_{T\text{-}PL}$= 196N, the radius of sliding surfaces r=0.05 m

F_{Dx0}=0; F_{Dz0}=0; F_x=F_{Dx0}; F_z=F_{Dz0}; γ_{120}=0; γ_{220}=0; γ_0=0 (hoverring).

The maximal wind= 7.62 m/s (27.4 km/h) was taken from the amplitude value of JAR-VLA sinusoidal wind for flight worthiness . The simple autopilod was used

$$F_x = F_{x0} + K_p x + K_d V_x \qquad (17)$$

Where K_p=-20 N/m and K_d= -10 N/(m/s). One can see (fig. 8) there is an significant static error, that isn't important in this case and may be liquidated as known by addition of an intergral member.

For the case of *hovering* without wind and encountering step wind disturbance $\begin{cases} W_z = 0 \text{ when } t < 6s \\ W_z = -7.62 \text{ m/s when } t > 6s \end{cases}$ and the same autopilot (17) we have some calculation results as follows (fig. 17, 18, 19,20):

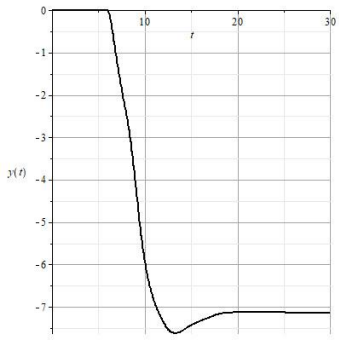

Figure 17. The deviation of the ballooncopter y(t) in the OX -axis when encountering wind, step disturbance

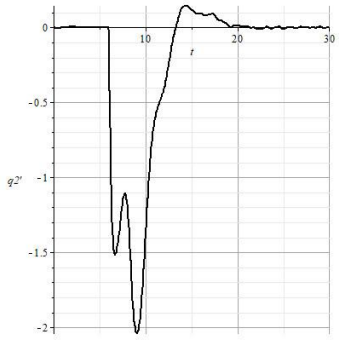

Figure 18. The deviation speed of the ballooncopter V_x(t) in the OX -axis when encountering wind, step disturbance

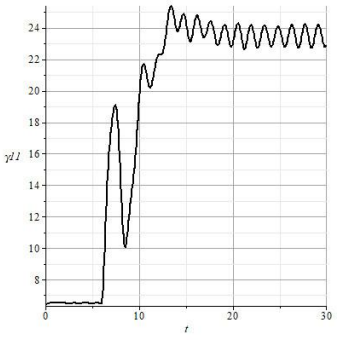

Figure 19. The oscillation angle of the multicopter γ_{12}(t) when encountering wind, step disturbance

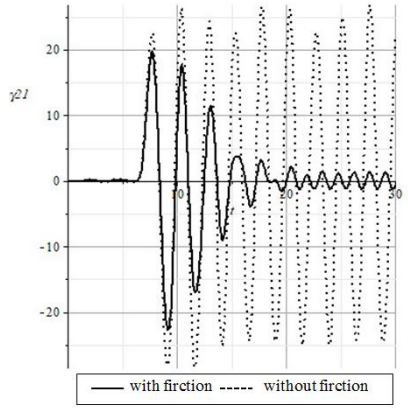

Figure 20. The oscillation angle of the payload $\gamma_{22}(t)$ when encountering wind step disturbance in cases : with / without friction.

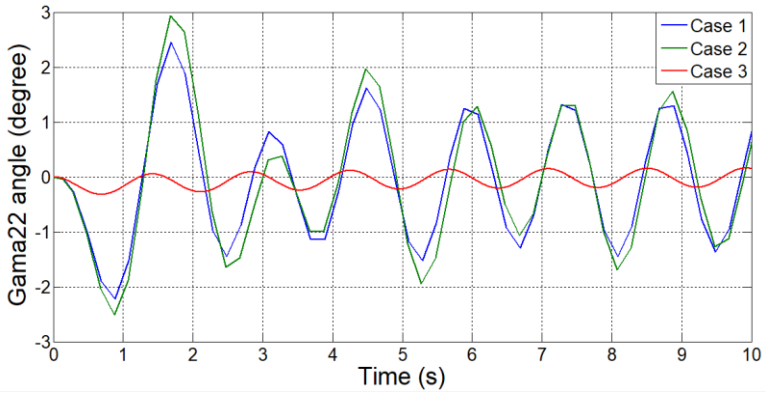

Case 1: L_2=1.5m; r=0.05m; Case 2: L_2=1.5m; r=0.03m; Case 3: L_2=0.05m; r=0.03m;

Figure 21. The oscillations of payload pendulum with different parameters of the pendulums and friction joint

One can see in case with friction (fig. 20) that the oscillations though became small but did not satisfy for monitoring. The further investigations shown on the fig.21 for 3 cases. The investigations were done by SIMULINK. Obviously that the case 3 (L_2 is decreased) has a very small amplitude that may satisfy the requirements for monitoring. In this case the radius r is also acceptable.

IV. CONCLUSION

This paper deals with the balloncopter with special assembly solution to hang the multicopter with the balloon and payload compartment according to the scheme of two pendulums suspended seriesly. This new assembly scheme has been considered for balance and stability in the scope of the flight and the hovering in the wind disturbances. The longitudinalal motion of the balloncopter is modeled by a 3-body, 4-degree-of-freedom system, and the motion law of the system is determined by the method of Lagrange II equations, the calculation is done in MAPLE. The software is accurately tested to determine its reliability when used as a design aid tool. The calculation results confirmed for a hypothetical balloncopters its flight dynamic stability in wind disturbance, including hovering flight. The joint for the payload in monitoring version must has intentional friction enough to damp the oscillations of the payload that is necessary to improve the infformations given by the payload. The authors suggest assumptions that there is no invers action to the whole 3-body mechanical system from the damped payload oscillations and the presence of static friction is neclected. In this case one can only predict the highest estimation of the oscillations that showed the possibility to completely damp the undesired oscillations with realistic parameters of the payload pendulum.

ABREVIATION

BC	Balloncopter
RS	Reference system
MC	Multicopter

BA	Balloon
PL	Payload
V_{xBA}, V_{zBA}	The x and z components of velocity of the balloon center in the ground reference system, [m/s]
V_{axBA}, V_{azBA}	The X and Z components of balloon aispeed (velocity of the center of balloon relative to the air), m/s
W_x, W_z	The X and Z components of wind speed in ground reference system, m/s
X_{BA}, Z_{BA}	The coordinates of the center of mass of the balloon in the ground reference system, m
G_{BL}	Ballast load (additional load to balance buoyancy), N
$G_{T\text{-}PL}$	Total payload (payload, payload compartment and ballast load), N
G_{SA}	Weight of balloon shell, N
G_{He}	Weight of helium gas, N
G_{BA}	Weight of balloon shell with helium gas, N
P_{ac}	Archimed's buoyancy force of the balloon, N
F_{EL}	Effective lift of the balloon, N
F_D	Aerodynamic force of the sphere, N
F_{Dx}, F_{Dz}	Projections of aerodynamic forces in the X, Z directions in the ground reference system OXZ, N
L_1	Length of suspension rod M_1M_2, m
L_2	Distance from suspension point M_{2d} to center of inertia M_3 or the radius of inertia of payload, m
D	Diameter of sphere, m
S	Cross-sectional area of sphere, m^2
$L_1'=L_1+R$	Distance OM_2, m
γ_0	Angle M_1OM_1', rad
γ_{12}	The angle from the vertical to the rod L_1, rad
γ_{22}	The angle from the vertical to the line L_2, rad
H	Current altitude of the balloon center , m
F_{x0}, F_{y0}	Initial forces of multicopter to maintain desired altitude H_d and desired speed V_d, N
C_x, C_z	The coefficient of aerodynamic drag of balloon in the X-axis and Z-axis (in the case of a sphere, $C_x=C_z$)
ρ_a, ρ_{He}	Density of air and helium, kg/m^3
M_{frx},	friction moment in the hang joint of the payload in the plane XM2Z, Nm
K_{fr}	Coefficient of sliding friction
R	Radius of sliding surfaces relative to the rotation center of the joint, m
N	Normal reaction of a sliding surface, N
F_i	Inertia force, N
M_i	Inertia force moment, Nm

REFERENCES

[1]. Nguyễn Đức Cương, Trần Duy Duyên và nnk - Mô tả sáng chế, "Phương tiện bay trực thăng nhẹ hơn không khí" Công báo Sở hữu công nghiệp số tháng 9/2021, Cục Sở hữu trí tuệ Việt Nam (Invention description published by Vietnam Intellectual Property Office).

[2]. Khoury, Gabriel Alexander (Editor), Airship Technology (Cambridge Aerospace Series), 2012, ISBN 0-521-60753-1. P.473.

[3]. Umberto Papa et al. Conceptual Design of a Small Hybrid Unmanned Aircraft System, Hindawi Journal of Advanced Transportation Volume 2017, Article ID 9834247, 10 pages (https://doi.org/10.1155/2017/9834247).

[4]. https://en.wikipedia.org/wiki/Drag_coefficient#/media/File:Drag_coefficient_on_a_sphere_vs._Reynolds_number_-_main_trends.svg

[5]. Đỗ Sanh: Cơ học tập 2, Nhà xuất bản Giáo dục, Hà Nội, 1998 (in Vietnamese).

[6]. Joint Aviation Requirements—Very Light Aircraft (JAR-VLA. pdf, Apr 26, 1990).

[7]. https://himya.ru/koefficient-treniya-tablicy-elektronnogo-spravochnika-po-ximii-soderzhashhie-koefficient-treniya.html(in Russian)